Heat Transfer through the Wairākei-Tauhara Geothermal System quantified by multi-channel data modelling

A. Ardid[1], R. Archer[1], E. Bertrand[2], F. Sepulveda[3], P. Tarits[4] and D. Dempsey[5]

[1] University of Auckland, Auckland, New Zealand.

[2] GNS Science, Lower Hutt, New Zealand.

[3] Contact Energy Ltd, Taupō, New Zealand.

[4] University of Western Britany, Plouzané, France.

[5] University of Canterbury, Christchurch, New Zealand.

Corresponding author: Alberto Ardid (aardids@gmail.com)

Key Points:

- Bayesian joint inversion of magnetotelluric and clay content data to infer the clay cap boundary
- Modeling of inferred clay cap and well temperature data to estimate clay formation temperatures and avoid misinterpretation of conductor nature
- Modeling of well temperature data to inferred thermal gradients and heat fluxes through the geothermal system

Abstract

To obtain the fullest picture of geothermal systems, it is necessary to integrate different types of data, e.g., surface electromagnetic surveys, lithology, geochemistry and temperature logs. Here, by joint modelling a multi-channel dataset we quantify the spatial distribution of heat transfer through the hydrothermally-altered, impermeable smectite layer that has developed atop the Wairākei-Tauhara system, New Zealand. Our approach involves first constraining magnetotelluric inversion models with methylene blue analysis (an indicator of conductive clay) and mapping these onto temperature and lithology data from geothermal wells. Then, one-dimensional models are fitted to the temperature data to estimate heat flux variations across the field. As a result, we have been able to map the primary seal that insulates the geothermal reservoir and estimate the heat flow of the system. The approach could be applied in geothermal provinces around the world with implications for sustainable resource management and our understanding of these magmatic systems.

1 Introduction

A geothermal system is a convective groundwater circulation system with three primary components: an underlying heat source, a fluid reservoir with sufficient permeability to support convective heat transport, and an overlying low permeability confining structure that is often formed from hydrothermally altered clays, commonly termed the clay cap. Given the clay cap's primary role to separate hot reservoir fluids from cold groundwater at shallow depths, constraining its geometry is a key component to developing conceptual models of geothermal systems that guide exploration, resource estimation, and operational decision-making. Although surface hydrothermal features are often associated with geothermal systems, subsurface geothermal reservoirs are obscured and their characterization (and sometimes discovery) relies on multidisciplinary surface exploration to reveal their location, size and temperature distribution (Cumming, 2009).

In electromagnetic geothermal prospecting, shallow conducive clay formations are synonymous with the shallow ‘conductor’. The magnetotelluric methods (MT) have emerged as the preferred technology for imaging this resistivity structure (Johnston et al., 1992), particularly for identifying drilling targets and improving the conceptual understanding of the deep geothermal system (Heise et al., 2008; Bertrand et al., 2015).

Hydrothermal alteration is used as a geothermometer in geothermal fields; the presence, degree of organization, and transitions between certain clay minerals indicate exposure of the rock to corresponding formation temperatures (Harvey and Browne, 1991) that could reflect either the contemporary temperature distribution, or relict activity. Titration analysis of drill cuttings using Methylene-Blue dye (MeB) is a method for estimating shallow conducive clay content (Gunderson et al., 2000) in smectite rich or interstratified illite-smectite formations (collectively referred to here as “smectite”). MeB profiles along well tracks can be used as a proxy for clay cap depth and thickness, and also as an indicator of temperature.

The Wairākei-Tauhara geothermal field is located on the northeast shore of Lake Taupō in the central Taupō Volcanic Zone (TVZ), New Zealand (Bibby et al., 1995). Wairākei-Tauhara is hosted in a deep, broad depression underlain by faulted greywacke basement and filled by low-density pyroclastic products and sediments (Bignall et al., 2010). The geothermal field reservoir is majorly contained in the permeable Waiora formation that comprises volcanic deposits with interlayered mudstones and sandstones; and the clay cap has known to be formed majorly in the Huka Falls Formation (HFF), a series of lacustrine sediments with particularly low permeability. Alteration mineralogy at Wairākei increases in rank and intensity with depth with smectite transforming to illite with increasing temperature through a series of progressively more ordered mixed-layer illite-smectite structures. Most of the argillic clay alteration occurs in the Huka Falls Formation (HFF) with some propylitic alteration in the lavas below. The heat output of the Wairākei-Tauhara geothermal system was estimated as ~530 MW by analysis of chloride fluxes, although large uncertainties are expected using this method (Fisher, 1964; Bibby et al., 1995).

Here, we present an integrated analysis of MT data, temperature logs, MeB profiles, and lithological information for the Wairākei-Tauhara geothermal field (Fig. 1). First, we use joint modeling of MT and MeB data (Ardid et al. 2020) to establish uncertain intervals for the upper and lower boundaries of the clay cap that vary across the field. Then, we interpolate temperature data across the clay layer to infer clay formation temperatures and gradients. Finally, using a 1-D heat and groundwater transport model (Bredehoeft and Papadopulus, 1965), we estimate heat flux through the clay cap and the heat output of the Wairākei-Tauhara geothermal system.

Integrating these multiple data sets provides a holistic and robust picture of the upper parts of a magmatic hydrothermal system. This approach helps to understand distributions of clay alteration in geothermal fields, how these relate to temperature and, by quantifying uncertainty, appropriate limits on inference. This step towards quantifying heat flow through a geothermal system can benefit understanding of the complex rifting tectonics in geothermal provinces in New Zealand, Iceland, and East Africa. From a practical perspective, an improved view of key hydrological structures and heat flow dynamics can also be used to constrain modeling and management of the geothermal resource.

2 Clay distribution from MT-MeB inversion

In 2010, an MT survey comprising 250 measurement sites (stations) was undertaken across the Wairākei-Tauhara geothermal field (Sepulveda et al., 2012) (Fig. 1). These data were used to generate resistivity inversion models to estimate the depth and thickness of a shallow conductive layer assumed to correspond to hydrothermal clays. The modelling used a Bayesian method (Ardid et al., 2020) that returns an ensemble of 1D three-layer models at each station, characterized by posterior distributions over two thickness and three resistivity parameters. A prior applied to the middle layer constrains its resistivity to a range typical for hydrothermal conductive clays (1-5 Ω m). Interpolating between the 1D models at each MT site builds a pseudo-3D geometry of the shallow conductivity structure in the geothermal field (Fig. 1A). By evaluating a range of models consistent with these data, we quantify our uncertainty in the clay cap geometry and carry this through subsequent analyses.

The MT inversion was constrained by a structural prior constructed from clay indications contained in fifty MeB profiles from well log data across the field (Fig. 1). This prior was imposed on the conductor boundaries but not the resistivity parameters. At each well, an ensemble of square functions is fitted to the MeB profile to capture the sharp appearance and disappearance of clay (Ardid et al., 2020). Then, a field-wide MeB prior is constructed by interpolating between ensembles at each well (see Supplementary material for details on uncertainty interpolation). Using MeB structural priors reduces the non-uniqueness of the MT inversion and is important for constraining the bottom boundary of the conductor, which can be smeared in common least-structure regularized MT inversion models (Ardid et al., 2020).

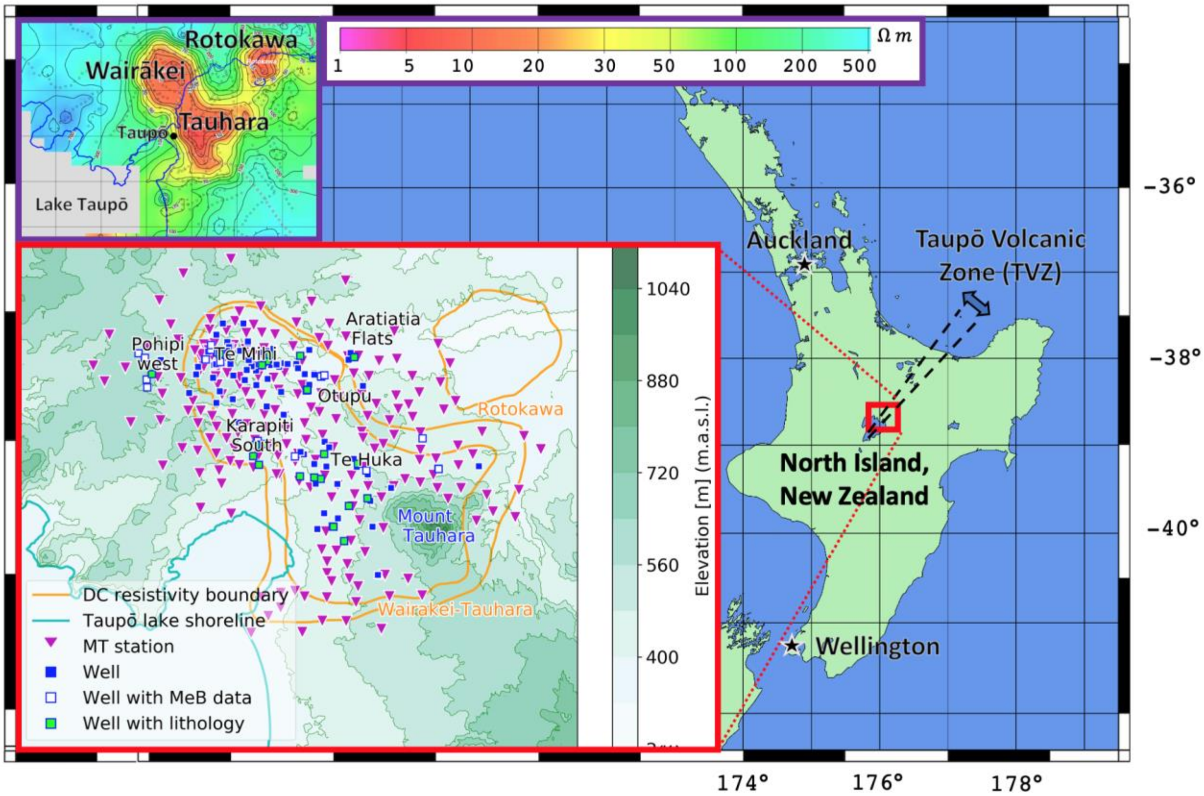

Figure 1. Map of the North Island of New Zealand, with location of the Taupō Volcanic Zone. The red square shows the Wairākei geothermal field, with the locations of magnetotelluric stations and wells, highlighting those with available lithology and methylene blue data. The background shows an elevation map and the Taupō Lake shoreline. Purple square shows the DC resistivity map (~250 m depth, Risk, 1984) with low-resistivity (red to orange colours) area delineating the inferred clay-cap of the Wairākei-Tauhara and neighboring Rotokawa Geothermal Fields.

Our MT inversion model results show that for the north and west areas of Wairākei, there is a good correlation between inferred clay layer and the shallow DC resistivity boundary (Fig. 2A). An exception is at Pohipi West where the presence of clay is inferred outside the DC resistivity boundary, likely due to relict clays observed at >300 m depth. (Sepulveda et al., 2012). However, the largest discrepancy is in the Aratiatia Flats region (Fig. 1) where the MT reveals deep conductor outside the conventional Wairākei boundary. The conductor here dips gently east and then plateaus at more than 400m depth where it abuts the nearby Rotokawa geothermal.

A 2D east-west section through the north of Wairākei (profile AA’ in Fig. 2A) reveals a mushroom-shaped low-resistivity layer inferred as a hydrothermal clay-cap (Fig. 3A), flattened near the surface in the center of the field and dipping away at the edges. The depth of this clay-layer largely correlates with the Huka Falls Formation, the primary aquiclude, as confirmed by stratigraphy and MeB profiles from four wells (WK124A, WKM14, WKM15 and WK317;

Figure 3A-B) located in the infield Te Mihi region (Fig. 1). The low permeability of the lacustrine sediments encourages formation of swelling clays at the high temperatures (~200°C) that occur in the geothermal upflow at Te Mihi (Sepulveda et al., 2012).

The lowest extent of the clay layer appears to correlate with the top of the Waiora Formation, notwithstanding the larger uncertainty attached to this boundary. Exceptions are at the field margins such as the Aratiatia Flats region east of the upflow where the clay layer deepens to be hosted in the Wairākei ignimbrite beneath the Waiora. Further east, it shallows toward the Rotokawa geothermal field suggesting a hydrothermal connection between the two fields. However, well data indicate low temperatures (Fig. 3B, well WK315B) and the conductor contained within the Wairakei ignimbrite. Ignimbrites under prolonged low-temperature regimes can undergo diagenetic alteration giving rise to conductive networks of clays and zeolite minerals (Bibby et al., 2005). This has been observed in the TVZ and has caused misunderstandings about the nature and genesis of the conductor (Bibby et al., 2005). Thus, consideration of the temperature data alongside the MT suggest the deep conductor plateau observed at the Aratiatia Flats region (Fig. 2A) is likely diagenetic and not hydrothermal alteration.

In the outfield west of Wairākei AA’, the conductor is absent (WT169a, Fig. 3A) and first appears in Pohipi West (WT006a, Fig. 3A). Inspection of temperature and well logs in the nearest well (WK681; Fig. 3) suggests no obvious stratigraphic or thermal control on the clay, which is formed in the volcanic alluvium and rhyolite (Fig. 3B). Cold temperatures suggest this is relict of past geothermal activity (Sepulveda et al., 2012). East of profile AA’ (outfield; Fig. 3A), the conductor deepens to well WK315B where clays occur in the Wairākei ignimbrite (Fig. 3A-B).

3 Thermal controls on clay presence

We used temperature profiles from 122 wells across the Wairākei-Tauhara field to investigate thermal constraints on clay formation. Interpolating data from wells close to profile AA’ indicates a modest correlation between infield isotherms and clay presence (Fig. 3A). Across the ~4 km span of the main upflow, between wells WK263 and WK317, the top and bottom clay boundaries correlate respectively with the 100°C and 180-200°C isotherms. On either side of this region, the 180°C isotherms dip sharply compared to the more gentle dip of clay presence, inferred from both resistivity and MeB data. So, in upflow high-temperature region – clay occurrence (i.e., low-resistivity) correlates well with expected smectite. But outside of upflow in low-temperature regions, clay still occurred but due to relict hydrothermal activity or caused by diagenesis in old ignimbrites (as discussed in the previous section).

We constructed distributions for upper and lower clay boundary temperatures across Wairākei-Tauhara from well temperature logs (Supplementary material). Regional temperature trends show the central upflow as the hottest part of the field, with cooling towards and outside the boundary (Fig. 2D). Average temperatures at the top and bottom of clay boundaries are 58°C and 199°C (Figs. 2E and 2F), consistent with expected the 50 to 200°C formation range for smectite and smectite-illite clays (Browne, 1978). They also corroborate with contemporary clay temperatures in geothermal fields in other regions, for example in Iceland (50 to 220°C; Arnason et al., 2000), Indonesia (~50 to 200°C ; Gunderson et al., 2000), Philippines (ambient to 230°C; Reyes et al., 1990), Kenya (~100 to 220°C; Lagat, 2013), Chile (90 to 190°C ; Maza et al., 2018) and El Salvador (~90 to 205°C ; Patrier et al., 1996). However, there is also substantial variability in the clay cap boundary temperatures, with a two-sigma median-centered range of ~ 20 to 120°C for the upper boundary and ~ 130 to 250 °C for the lower boundary (Figs. 2E and 2F). This variability suggests that correlation between clay formation and temperature need to be interpreted cautiously (particularly where clay presence is inferred from geophysics and not confirmed by wells).

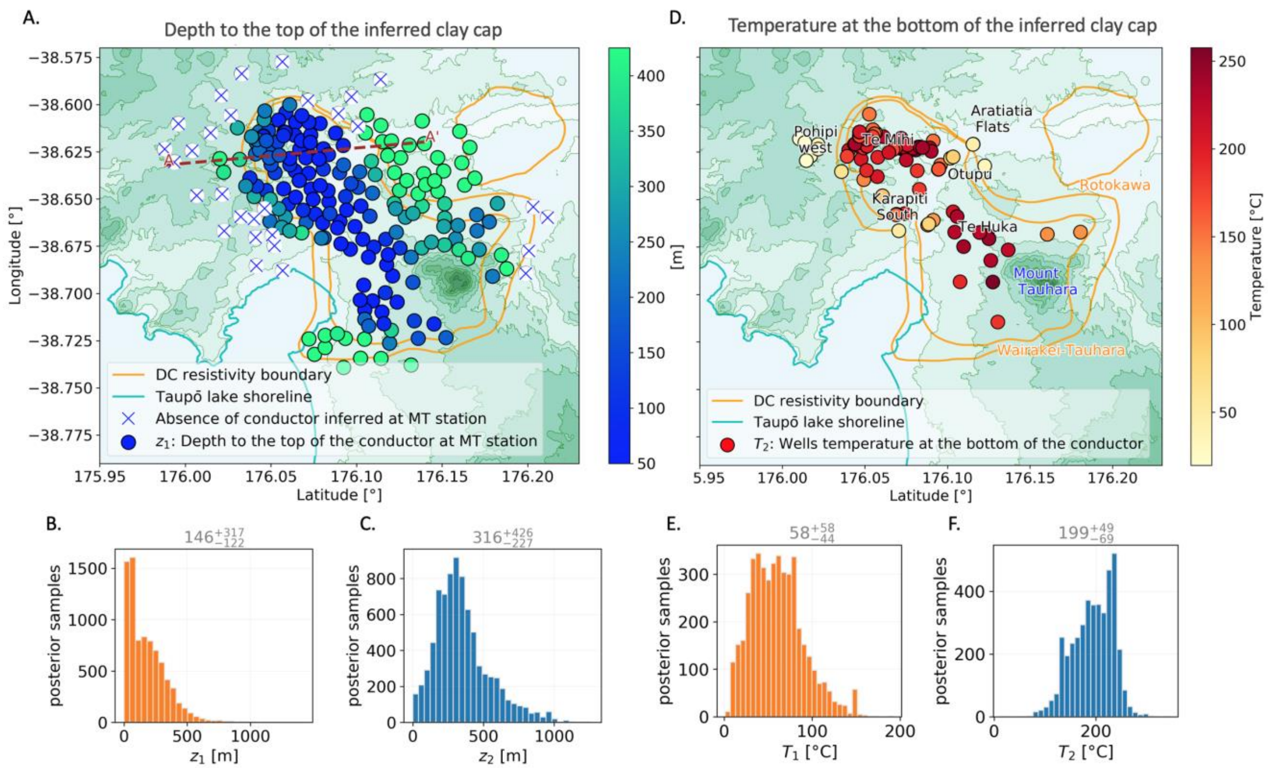

Figure 2. (A) Scatter circles show the mean 1D inverted depth to the top of the clay cap at the location of magnetotelluric (MT) stations. Crossed circles indicate locations where a shallow conductor (i.e., clay-cap) was not imaged by the MT data. Orange lines indicate the boundary of the Wairākei-Tauhara geothermal field. Black dots indicate wells where methylene blue (MeB) profiles were available. The background shows an elevation map and the Taupō Lake shoreline. (B) and (C) show histograms for infield depths to the top of the conductor (z_1) and conductor thickness (z_2) for the inverted MT data. (D) Scatter circles show the temperature at the bottom of the inferred clay cap in well locations, along with the DC resistivity boundary for the Wairākei-Tauhara geothermal field. (E) and (F) show histograms for the temperature samples at the top and the bottom of the conductor from temperature well data (T_1 and T_2 respectively). Note: ZZ^{xx}_{yy} indicates two-sigma distribution where the interval [xx, yy] contains 95% observations centered at the median ZZ.

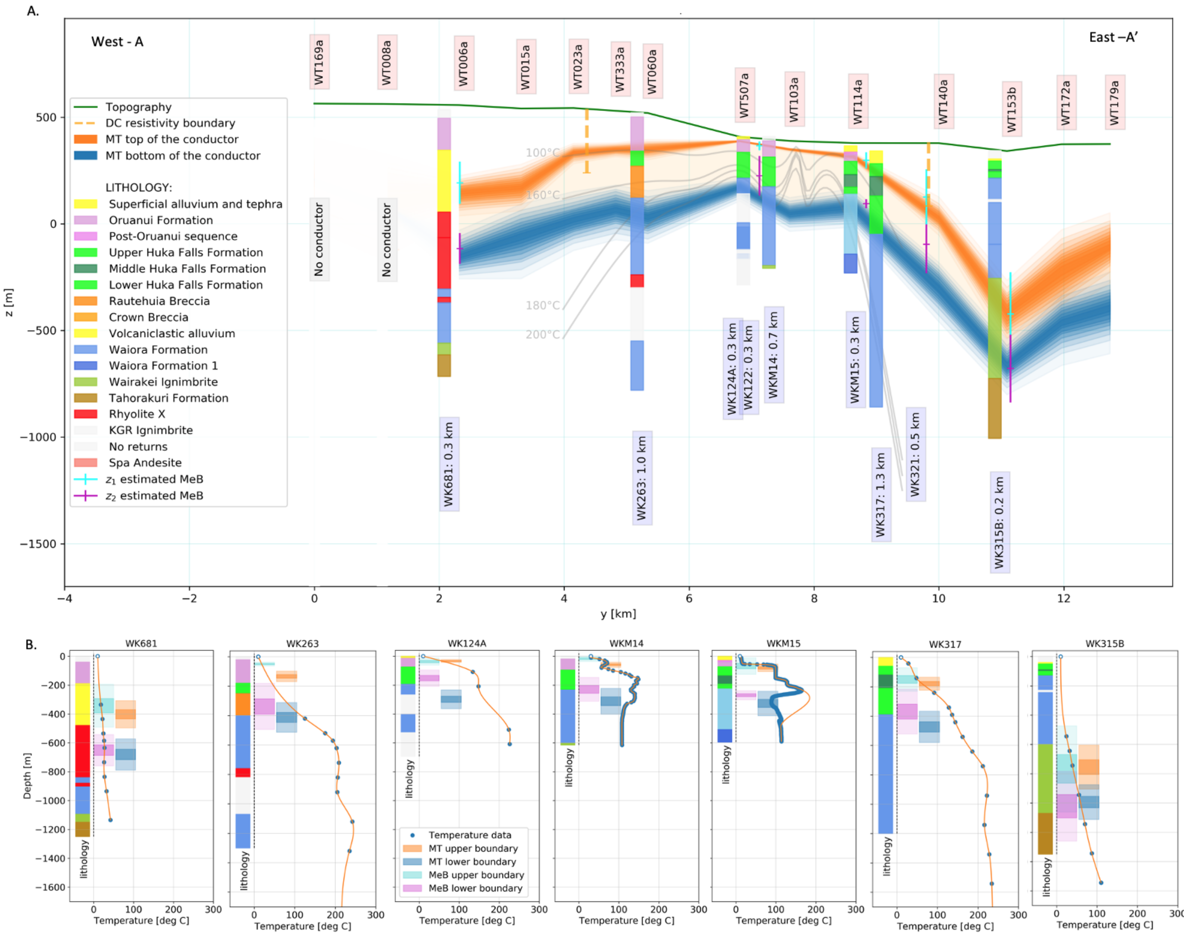

Figure 3. (A) Profile A-A' (Fig. 2A) showing the inferred clay cap boundaries derived from 1D magnetotelluric (MT) inversion models, along with estimates of clay distribution estimated from methylene blue data (MeB) in wells (used as prior distributions for the MT inversion). Temperature isotherms (grey contours) interpolated from wellbore measurements using cubic spline. Lithology for some of the wells close to the profile are also shown. MT locations and station names are shown as red boxes (top) and well locations and names as blue boxes (bottom) with perpendicular distance to the profile. Interception of the profile with the resistivity boundary is indicated by vertical dashed orange lines to a depth of 300 m. (B) Shown from left to right for seven wells along the profile are: stratigraphy, inferred clay distribution from MeB data, inferred clay cap boundaries from MT inversion, and the well temperature profile.

4 Geothermal gradient and heat flux through the clay cap

Using clay cap thicknesses and boundary temperature inferences, we computed effective linear temperature gradients across the field, which had a two-sigma distribution of $476\pm^{175}_{336}$ °C/km (Fig. 4B). For a typical thermal conductivity gradient of 2.2 W/m°C, this corresponds to a conductive heat flux of $1.05\pm^{0.15}_{0.22}$ W/m^2. Conductive heat flux and temperature gradient show a similar trend to clay boundary temperatures (Fig. 3), with the highest values (~700 °C/km, 1.54 W/m^2) in the Te Mihi area (Fig. 1) and lowest values (<300 °C/km, 0.7 W/m^2) in the outfield areas of Pohipi West and Aratiatia Flats. By interpolating between conductive heat fluxes calculated at wells with inferred values at the field boundary, we estimated the conductive heat flow for the Wairakei field as ~153±18 MW.

We constructed an improved model for vertical heat transfer by also considering advection, which is the heat transported by upwelling of hot water through the clay cap. In steady state, advection imposes an exponential deviation on the linear conductive temperature gradient (Bredehoeft and Papadopulus, 1965)

$$T = (T_L - T_0)\frac{e^{\beta z/L} - 1}{e^{\beta} - 1} + T_0, \qquad \beta = \frac{c\rho v_z L}{\kappa} \qquad (1)$$

where β is a dimensionless parameter that depends on specific heat and density of water, c and ρ, vertical flow velocity, v_z, effective thermal conductivity of the layer, κ, and thickness of the clay layer, L, with upper and lower temperatures T_0 and T_L. This 1D model is appropriate for our system because the clay cap is sub-parallel to the surface, and fluid velocity is expected to be primarily vertical, driven by buoyant upwelling

Fitting an analytical model of this form to each well's temperature data in the inferred clay depth range (Supplementary material), we estimated the vertical heat flux through this unit. Across the field, the distribution of vertical clay cap heat fluxes was ~ $2.15\pm^{5.9}_{1.3}$ W/m^2 (Fig. 4C) with a total estimated heat flow for the field of 380 ± 21 MW (Fig. 4E). The largest contribution is concentrated around the production zones at Te Mihi, south of Te Huka, and north of Mt. Tauhara.

We interpret the total heat flow through the clay cap as a lower bound on the total heat flow of the geothermal system, which historically has proven difficult to quantify (Fisher, 1964; Bibby et al. 1995). Notably, this estimation does not consider heat that escapes the reservoir via lateral outflows below the clay cap or through localized high-permeability pathways whose thermal signature has not been sampled by nearby wells. These pathways that may feed localized surface features like geysers or mud pools could represent substantial heat flow, e.g., Fisher (1964) estimated ~200 MW of surface heat loss by surface features. Previous estimates of Wairākei-Tauhara heat output (~530 MW; Bibby et al., 1995) based on geochemical considerations are about 40% higher than ours. However, high uncertainties are expected for chlorate-ratio methods estimated on ~25%, where the overall accuracy is difficult to judge (Bibby et al., 1995). On the other hand, our method has several advantages over prior estimates in that it directly utilizes observations of wellbore temperatures and geometrical constraints on the clay cap from MT and MeB data. Many well-characterized fields have temperature and MT data, so a similar method can be applied. Nevertheless, at an early exploration phase geochemistry based methods may be preferred until MT and temperature data are available.

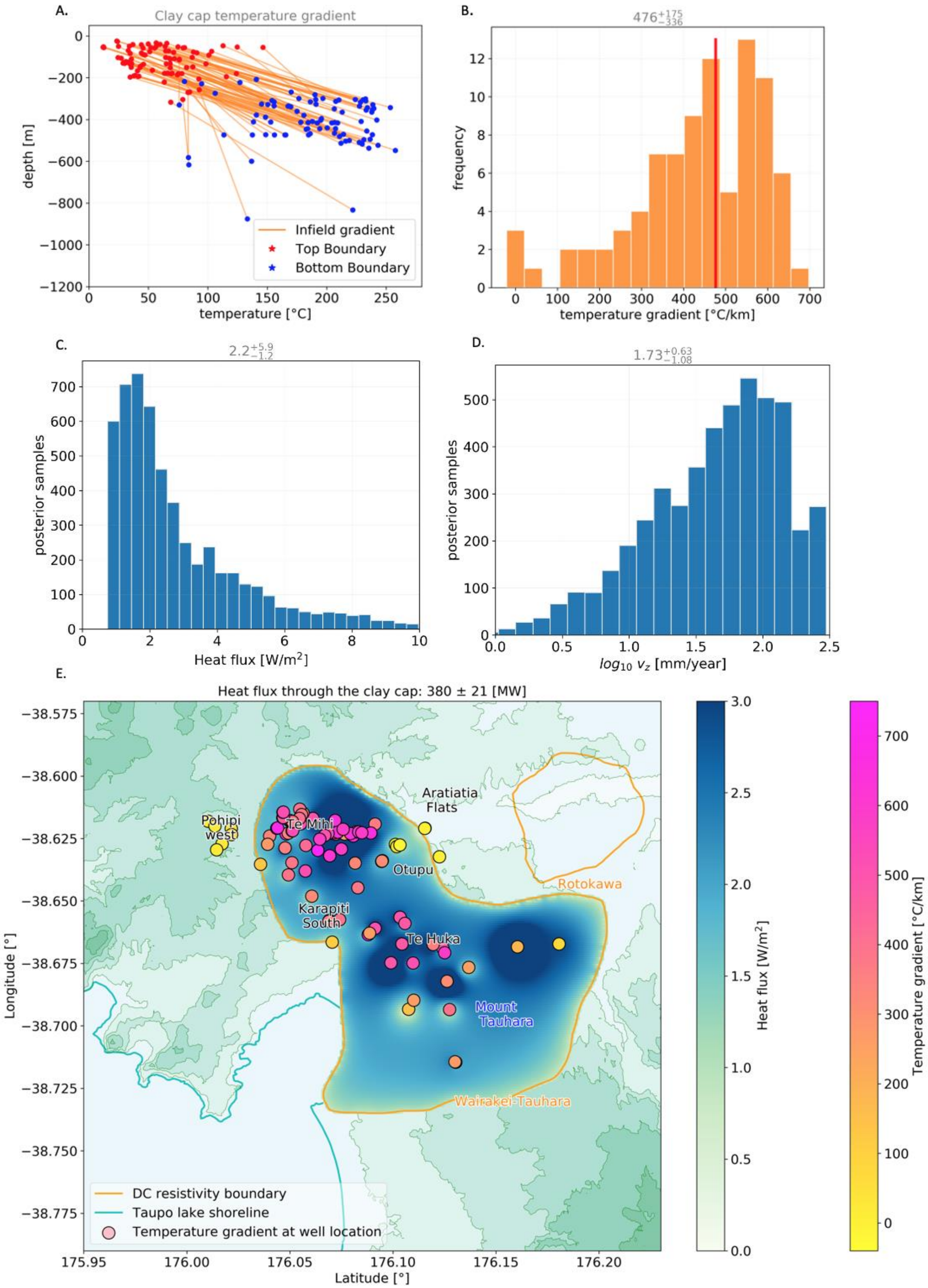
A.
Clay cap temperature gradient
depth [m]
temperature [°C]
Infield gradient
Top Boundary
Bottom Boundary
B.
476$^{+175}_{-336}$
frequency
temperature gradient [°C/km]
C.
2.2$^{+5.9}_{-1.2}$
posterior samples
Heat flux [W/m^2]
D.
1.73$^{+0.63}_{-1.08}$
posterior samples
log_{10} v_z [mm/year]
E.
Heat flux through the clay cap: 380 ± 21 [MW]
Pohipi west
Te Mihi
Aratiatia Flats
Otupu
Rotokawa
Karapiti South
Te Huka
Mount Tauhara
Wairakei-Tauhara
DC resistivity boundary
Taupo lake shoreline
Temperature gradient at well location
Longitude [°]
Latitude [°]
Heat flux [W/m^2]
Temperature gradient [°C/km]

246

Figure 4. (A) Red and blue dots show the inferred depth and observed temperature at the top and bottom of the clay cap, respectively. Orange lines connecting the top and bottom dots of the same well show the linear temperature gradient through the inferred clay cap. (B) Histogram showing the distribution of temperature gradients with the median value indicated by the red bar. (C) Posterior samples of heat flux modelled by 1D conduction-advection model fit to temperature logs (Eq. (1)). (D) Posterior samples of upward fluid velocity through the clay cap derived from β estimations (supplemental material, Eq. (1)). (E) Map of linear temperature gradients described in (A). The background shows the estimated natural state heat flux through the clay cap for the geothermal field interpolated from well samples in (C).

In estimating heat flow using the exponential model, we have assumed that the temperature distribution within the clay cap is similar to the steady-state temperature distribution prior to development of the geothermal system that began in the 1950s. These activities include extraction and reinjection of fluids from the main reservoir, which can disturb the flow field and encourage cold water inflows. Given the ~ 60 year history of energy production at Wairākei, some perturbation of the natural state temperature distribution is expected, particularly in the reservoir beneath the clay cap. We estimated the extent to which temperature disturbances above or below the clay cap would propagate into this layer by conduction alone. The thermal diffusion length scale is commonly given as $L = \sqrt{\alpha\tau}$, where α is thermal diffusivity (10^{-6} m^2/s for most rocks) and τ is the length of the temperature disturbance (up to 60 years of production). A penetration length scale of ~43 m is obtained. In other words, temperatures at the bottom boundary of the clay cap, if disturbed by Wairākei production activities that encourage cold water inflows, will only have been disturbed in the first 43 m. This is only ~14% of the average 316 m clay layer thickness and so is unlikely to have a first order influence on temperature profiles and heat fluxes derived from them.

From the β distribution calculated from (1) at wells, we were able to estimate the upward fluid velocity through the clay cap to a value of ~ $53\pm_{49}^{175}$ mm/year (Fig. 4D). This low value reflects the impermeable character of the clay cap, and is consistent with the 30 to 80 mm/year rate estimated for fluids rising by convection in the brittle crust (Weir, 2009).

5 Summary

We have presented a multidisciplinary analysis of the extent, stratigraphic context, and thermal structure of the hydrothermally altered clay layer in the Wairākei-Tauhara geothermal system, New Zealand. Using an MT inversion constrained by MeB clay indications, we have imaged a 300 m thick conductive layer reflective of the clay cap that tracks the primary aquiclude (Huka Falls Formation) overlying a distinct reservoir unit (Waiora Formation). Mapping well temperature and lithology data into this structure allowed us to differentiate contemporary from relict clays and diagenetic alteration. Misinterpretation of the conductor nature could lead to a dud well (~10M USD drilled well that encounters dry and low-temperature conditions. Dub wells could impact significantly the return investment on geothermal exploration projects). Also, by mapping well temperature on the conductor revealed by the MT-MeB inversion we confirms a broad range of smectite formation temperatures between $59\pm_{45}^{56}$ °C and $198\pm_{69}^{48}$ °C. Applying simple heat transfer models through the clay cap, whose temperature distribution has likely been preserved post human exploitation, indicates a lower bound of 380±21 MW for the total system heat flow.

Quantifying heat flow through geothermal systems can help us understand the upper crustal magmatism that drives them (e.g., Rowland et al., 2010). For example, the estimated heat flux average of 2.5 W/m2 (ranging from 1 to 7 W/m2) focused through the field is assumed to be balanced at 6 to 8 km depth by a much broader heat sweep at the convection cell base (Wooding, 1978). Combined with catchment estimates four to seven times larger in area than the geothermal fields themselves (Dempsey et al., 2012), this corresponds to heat extraction from buried magma reservoirs between 0.3 and 0.6 W/m2. Regional modelling of coupled magmatic-geothermal systems like the Wairākei-Tauhara-Rotokawa complex is a promising tool for investigating how heat transfer indicates or modulates volcanism (Tramontano et al., 2017) at calderas such as Taupō, and the areal heat flows presented here will help constrain those models.

Modelling is also used to track the short-term evolution of geothermal reservoirs to optimize electricity generation (e.g., O'Sullivan et al., 2009). Reservoir models are constrained by temperature and pressure measurements at isolated well locations, which leads to an ill-posed calibration problem. However, field-wide inferences of first-order permeability structures like the clay cap and its heat flux distribution could be used to reduce non-uniqueness and thus improve model derived predictions. In this regard, geophysical surveys are complementary to traditional datasets because they represent a relatively low-cost method to sample large crustal volumes that are not directly sampled by wells.

The methodologies introduced could be applied to improve understanding in complex tectonic rifts as Iceland and East Africa, and geothermal provinces as Indonesia, Philippines, Japan, Central and South America, among others. Future directions for this research could include other subsurface resource estimation in other fields where drilling is available. For instance, when inferring the geometry of groundwater reservoirs from EM geophysical surveys, priors could be developed from drilling outputs like water content or lithology, or salinity profiles in offshore aquifers. Or, repeated sampling at semi-permanent MT stations combined with time-series borehole data, could be used to introduce a time dimension to the inversions. This sets the stage for near real-time reservoir monitoring and, possibly, short-term predictive modelling.

Acknowledgments

Contact Energy Ltd. is thanked for data support and permission to publish data. The authors also thank funding from the Ministry for Business, Innovation and Employment from New Zealand through the Empowering Geothermal and Dumont d'Urville grants and the Faculty of Engineering at the University of Auckland.

References

Arnason, K., Karlsdottir, R., Eysteinsson, H., Flovenz, O. G., &Gudlaugsson, S. T. (2000), The resistivity of high-temperature geothermal systems in Iceland: *Proceedings, World Geothermal Congress 2000, Kyushu - Tohoku, Japan*

Ardid, A., Dempsey, D., Bertrand, T., Tarits, P. & Archer, R. (2020), Bayesian magnetotelluric inversion using structural priors for imaging shallow conductors in geothermal fields: GEOPHYSICS (in press).

Bertrand, E.A., Caldwell, T.G., Bannister, S., Soengkono, S., Bennie, S.L., Hill, G.J., & Heise, W. (2015), Using array MT data to image the crustal resistivity structure of the southeastern Taupo Volcanic Zone, New Zeland: *Journal of Volcanology and Geothermal Research*, v. 305.

Bibby, H.M., Caldwell, T.G., Davey, F.J., & Webb, T.H. (1995), Geophysical evidence on the structure of the Taupo Volcanic Zone and its hydrothermal circulation: *Journal of Volcanology and Geothermal Research*, v. 68, p. 29–58, doi: 10.1016/0377-0273(95)00007-H.

Bibby, H.M., Risk, G.F, Caldwell, T.G. & Bennie, S.L. (2005), Misinterpretation of Electrical Resistivity Data in Geothermal Prospecting: a Case Study from the Taupo Volcanic Zone: *Proceedings, World Geothermal Congress 2005, Turkey*.

Bignall, G., Milicich, S.D., Ramirez, L.E., Rosenberg, M.D., Kilgour, G.N., & Rae, A.J. (2010), Geology of the Wairakei-Tauhara geothermal system, New Zealand: *Proceedings, World Geothermal Congress 2010, Indonesia*.

Bredehoeft, J.D., & Papadopulos, I.S. (1965), Rates of vertical groundwater movement estimated from the earth's thermal profile: *Water Resources Research*, v. 1, p. 325-328, doi: 10.1029/WR001i002p00325.

Browne, P.R.L. (1978), Hydrothermal alteration in active geothermal fields: *Annual Review of Earth and Planetary Sciences*, v. 6, p. 229-250, doi: 10.1146/annurev.ea.06.050178.001305.

Cumming, W. (2009), Geothermal resource conceptual models using surface exploration data: *Proceedings, 34th Workshop on Geothermal Reservoir Engineering, Stanford University*.

Dempsey, D.E., Simmons, S.F., Archer, R.A., & Rowland, J.V. (2012), Delineation of catchment zones of geothermal systems in large-scale rifted settings: *Journal of Geophysical Research*, v. 117, doi:10.1029/2012JB009515.

Fisher, R.G. (1964), Geothermal heat flow at Wairakei during 1958: *New Zealand journal of geology and geophysics*, v.7, p. 172-184, doi: 10.1080/00288306.1964.10420168

Gunderson, R., Cumming, W., Astra, D., & Harvey, C. (2000), Analysis of Smectite Clays in Geothermal Drill Cuttings by the Methylene Blue Method: For Well Site Geothermometry and Resistivity Sounding Correlation: *Proceedings, World Geothermal Congress 2000, Japan*.

Harvey, C. & Brown, P.R.L. (1991), Mixed-Layer Clay Geothermometry in theWairakei Geothermal Field, New Zealand: *Clays and Clay Minerals*, v. 39, p. 614–621, doi: 10.1346/CCMN.1991.0390607.

Heise, W., Caldwell, T.G., Bibby, H.M., & Bannister, S.C. (2008), Three-dimensional modelling of magnetotelluric data from the Rotokawa geothermal field, Taupō Volcanic Zone, New Zealand: *Geophysical Journal International*, doi: 10.111/j.1365-246X.2008.03737.x.

Johnston, J.M., Pellerin, L., & Hohmann, G.W. (1992), Evaluation of electromagnetic methods for geothermal reservoir detection: *Geothermal Resources Council Transactions*, v. 16, p. 241-245.

Lagat, J. (2013), Hydrothermal alteration mineralogy in geothermal fields with case examples from Olkaria Domes Geothermal Field, Kenya: Presented at *Short Course VIII on Exploration for Geothermal Resources*, https://orkustofnun.is/gogn/unu-gtp-sc/UNU-GTP-SC-11-02.pdf

Maza, S., Collo, G., Morata, D., Lizana, C., Camus, E., Taussi, M., & Rivera, G. (2018), Clay mineral associations in the clay cap from the Cerro Pabellón blind geothermal system, Andean Cordillera, Northern Chile: *Clay Minerals*, v. 53, n. 2, p. 117-141, doi:10.1180/clm.2018.9.

O'Sullivan, M.J., Yeh, A., & Mannington, W.I. (2009), A history of numerical modelling of the Wairakei geothermal field: *Geothermics*, v. 38, doi:10.1016/j.geothermics.2008.12.001.

Patrier, P., Papapanagiotou, P., Beaufort, D., Traineau, H., Bril, H., & Rojas, J. (1996), Role of permeability versus temperature in the distribution of the fine (< 0.2 μm) clay fraction in the

Chipilapa geothermal system (El Salvador, Central America): *Journal of Volcanology and Geothermal Research*, v. 72, doi: 10.1016/0377-0273(95)00078-X.

Reyes, A.G. (1990), Petrology of Philippine geothermal systems and the application of alteration mineralogy to their assessment: *Journal of Volcanology and Geothermal Research*, v. 43, doi: 10.1016/0377-0273(90)90057-M.

Risk, G. F. (1984), Electrical resistivity survey of the Wairakei geothermal field: *Proceedings, 6th New Zealand Geothermal Workshop*, p. 123-128.

Rowland, J.V., Wilson, C.J.N., & Gravley, D.M. (2010), Spatial and temporal variations in magma-assisted rifting, Taupō Volcanic Zone, New Zealand: *Journal of Volcanology and Geothermal Research*, v. 190, p. 89–108, doi: 10.1016/j.jvolgeores.2009.05.004.

Sepulveda, F., Glynn-Morris, T., Mannington, W., Charroy, J., Soengkono, S., & Ussher, G. (2012), Integrated approach to interpretation of magnetotelluric study at Wairākei, New Zealand: *36th Workshop on Geothermal Reservoir Engineering, Stanford University*.

Tramontano, S., Gualda, G.A.R., & Ghiorso, M.S. (2017), Internal triggering of volcanic eruptions: tracking overpressure regimes for giant magma bodies: *Earth and Planetary Science Letters*, v. 472, doi:10.1016/j.epsl.2017.05.014.

Ussher, G., Harvey, C., Johnstone, R., & Anderson, E. (2000), The resistivity structure of high-temperature geothermal systems in Iceland*: Proceedings, World Geothermal Congress 2000, Japan.*

Weir, G.J. (2009), A mathematical model of rainfall-controlled geothermal fields: *Transport in Porous Media*, v. 77, p. 323–334, doi: 10.1007/s11242-008-9312-y.

Wooding, R. A. (1978), Large-scale geothermal field parameters and convection theory: *Proceedings, 2th Workshop Geothermal Reservoir Engineering, Stanford University*.